Photography," *J. Soc. Motion Picture Television Eng.*, **80**, 951 (1971).
Perry, M. G., and M. F. Handley, "The Dynamic Arch in Free Flowing Granular Material Discharging from a Model Hopper," *Trans. Ins. Chem. Eng.*, **45**, 367 (1967).
Reddy, K. VS., M. C. Van Wijk, and D. C. T. Pei, "Stereophoto-Grammetry in Particle-Flow Investigation," *Can. J. Chem. Eng.*, **47**, 85 (1969).
Richards, Bryan E., ed., *Measurement of Unsteady Fluid Dynamic Phenomena*, Hemisphere Publishing Corp. (1977).
Schichtin, H., *Boundary Layer Theory*, McGraw Hill Book Co., NY, 6th ed., 106 (1968).
Self, S. A., and J. H. Whitelaw, "Laser Anemometry for Combustion Research," *Combustion Sci. and Tech.*, **13**, 171 (1976).
Soo, S. L., *Fluid Dynamics of Multiphase Systems*, Blaisdell Publishing Co. (1967).
Stümke, A., and H. Umhauer, "Local Particle Velocity Distributions in Two-Phase Flows Measured by Laser-Doppler Velocimetry," Dynamic Flow Conference, Marseille (Sept., 1978).
Vardelle, A., M. Vardelle, J. M. Baronnet, and P. Fauchais, "Particles Velocity and Temperature Statistical Measurements in a d.c. Plasma Jet," 4th International Symposium on Plasma Chemistry, Zürich (Aug. 27-Sept. 1, 1979).

Manuscript received March 3, 1980; revision received July 17, and accepted July 25, 1980.

Drag Force Measurement of Single Spherical Collectors with Deposited Particles

HEMANT PENDSE
CHI TIEN
and
R. M. TURIAN

Department of Chemical Engineering and Materials Science
Syracuse University, Syracuse, New York 13210

The hydrodynamic drag force in a uniform flow field acting on a spherical body with small particles attached to its surface was determined experimentally. The experimental data are used to substantiate the approximate force expressions derived from available theories for several types of collector-particle geometries. Procedures for applying these results to the prediction of the pressure drop across a filter bed with various degrees of particle deposition are also developed.

SCOPE

Determination of the drag force acting on a spherical body with a number of smaller spheres attached to it is a very important problem in hydrodynamics, and because of its inherent complexity, it has been the subject of a number of investigations in the past. The purpose of this work was to examine the body of available results relating to this flow, to evaluate in detail their efficacy as practical means for predicting the drag force (i.e., over and above their representations as formal approximate mathematical solutions), to devise effective computational procedures appropriate to each, and to generate experimental data capable of providing critical tests of these results. The ultimate result of these tests was to develop accurate, yet relatively simple, procedures for estimating the drag force for creeping flow past such groups of spheres.

CONCLUSIONS AND SIGNIFICANCE

The drag force acting on a spherical body with a number of smaller spheres attached to it is basic to understanding deep bed filtration. The results of previous works have indicated the relevance of this flow to deep bed filtration, particularly in regard to determining the increase in pressure drop as the filter becomes progressively clogged. Principally, previous work has demonstrated that idealizing the filter grain by an equivalent spherical collector provided a convenient, yet sufficiently realistic, representation of the overall filtration process. In addition, calculations have indicated that the process of particle deposition within the filter progressed according to three main stages: a particle to grain deposition phase, followed by a dendritic growth phase, and concluding with a phase in which the deposition process is dominated by the consequences of interaction among dendrites. The significance of calculations of the drag forces for various configurations of sphere groupings corresponding to these stages of filtration is therefore evident, since they form the basis for predicting the relationship between the pressure drop across the filter with the degree of particle deposition.

R. M. Turian is presently with the Department of Energy Engineering, University of Illinois at Chicago Circle, Chicago, Illinois 60680. H. Pendse is with the Department of Chemical Engineering, University of Maine, Orono, Maine 04473.

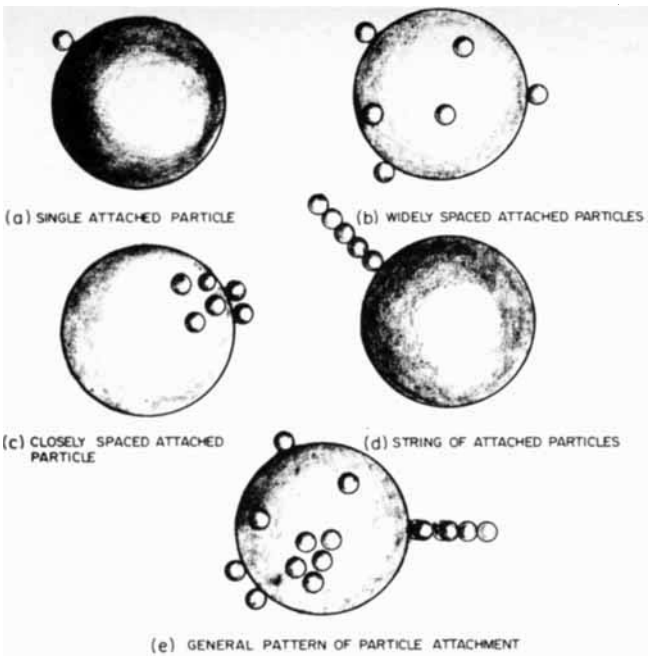

Figure 1. Types of collector-particle assemblies.

The purpose of the present work is to develop accurate, yet relatively simple procedures which can be used to estimate the hydrodynamic drag force, under creeping flow conditions, acting on a spherical body with a number of smaller spheres attached to it. The practical motivation for the study derives from its relevance to deep bed filtration, namely to the prediction of the increase in pressure drop as the bed becomes increasingly clogged. Because the increase in pressure drop is often the main factor determining the length of the filtration cycle, an understanding of the clogging phenomenon, or more importantly the prediction of pressure drop as a function of the extent of clogging (i.e., the amount of particulate matter retained) is of obvious importance.

The pressure drop associated with the flow of a fluid through a porous medium can be calculated, in principle, from the drag force acting on the surfaces of the medium matrix. However, for deep beds of granular substances, it has been found convenient to model the filtration process using the single-shere model, whereby each filter grain is viewed as a spherical collector. The retention of particulate matter in a filter bed results from the attachment of small particles on the filter grains. Thus, the measurement of the drag force acting on a spherical body with small particles attached to it pertains to a model system suitable for the study of the pressure drop increase in a clogged filter.

The dynamics of particle deposition in deep bed filtration is a complex process, which still presents formidable problems in spite of the many studies carried out during recent years. Beizaie (1977), employing a simulation technique developed by Tien et al. (1977), suggested that deposition could be viewed to consist of three stages. During the initial, clean collector stage deposition results in the attachment of particles to the collectors at discrete points on the collector surface. The second stage, designated as the dendrite growth stage, is characterized by an increased level of deposition from the attachment of particles from suspension onto particles deposited earlier; thus, resulting in the formation of particle dendrites. During the final stage, described as the open-structured, solid growth stage, adjacent particle dendrites (both from the same collector and from neighboring collectors) become entangled and intermeshed; particle collection is entirely due to the deposition on deposited particles.

The geometric configuration of the situations considered in this study can be classified according to the several types shown in Figure 1. Figures 1(a), 1(b), and 1(c) represent respectively the attachment of a single particle, several particles with relatively large distances between adjacent particles, and several particles close to each other on the spherical collector surface. These correspond to the evolution of deposit morphology during the initial (or clean collector) stage. Figure 1(d) shows an ideal particle dendrite attached to a spherical collector. An ideal dendrite is a string of attached particles whose centers lie on a straight line passing through the center of the sphere as defined by Payatakes and Tien (1976). A general situation is depicted in Figure 1(e), which can be viewed as a composite of types (a) and (d). One can, therefore, estimate the drag force acting on a collector with deposited particles from the contributions of the individual deposited particles of these two types, provided that the effect of possible interactions of neighboring deposited particles is taken into account. This is the approach used in the present work.

The present study consists of two parts. In the first part, semi-empirical expressions based on multiparticle low Reynolds number theory for the estimation of the drag force on spherical-particle assemblies of the various types, such as those shown in Figure 1, are proposed. In the second part, we examined the results of experiments conducted to test these expressions.

ESTIMATION OF DRAG FORCE CONTRIBUTIONS OF ATTACHED PARTICLES

A significant body of published work on the problem of creeping flow over a collection of spherical bodies arranged according to different geometries exists, which can be viewed as extensions of the classical Stokes solution (Stokes, 1851) for creeping flow over a single sphere. Application of these existing theories to the problems considered in the present study, however, was not successful because of a variety of reasons. For example, the analytical method with the use of the bipolar coordinates, which has been successfully applied to the solution of two-spheres problem (Stimpson and Jeffery, 1926; Goldman, Cox and Brenner, 1966; O'Neil, 1969; Lin, Lee and Sather, 1970; Nir and Acrivos, 1973) is not applicable to a cluster of more than two particles. Similarly, the method of reflections (Happel and Brenner, 1973) was found to break down if the size ratio of the attached particle to the collector is too small. A detailed account in the review of this topic is given by Pendse (1979).

The expressions for drag force contribution presented below are derived from intuitive application of certain theoretical results. While they may lack mathematical rigor, their utility is based on their ability to predict experimental data with sufficient accuracy as shown in later sections of this paper.

Single Attached Particle

For the case of a single particle attached to a spherical collector, an approximate estimate of the drag force acting on the attached particle can be obtained using Faxen's law (Happel and Brenner, 1973). Faxen's law states that for a stationary sphere immersed in an arbitrary flow, given as $\overline{V} = \overline{V}(\overline{r})$, the drag force acting on the sphere is found to be:

$$\overline{F}_D = 6\pi\mu a\left[\overline{V}_{(o)} + \frac{a^2}{6}\left(\nabla^2 \overline{V}_{(o)}\right)\right] \tag{1}$$

where the subscript (o) designates that the quantity is evaluated at the center of the sphere, and a is the radius of the sphere, when $\overline{V}(\overline{r}) = U\overline{i}_z$, Eq. 1 yields $\overline{F}_D = (6\pi a\mu U)\,\overline{I}_z$, which is the same result given by Stokes law.

As a simple illustration, consider the problem of a stationary sphere of radius 'a' placed in a cylindrical tube of radius 'R_o' through which a viscous fluid is moving. Let the cylinder axis be the Z axis, the sphere center be placed at a distance $R = \beta$ from this axis and U_o be the undisturbed fluid velocity at the tube axis. The undisturbed flow field is given by:

$$\overline{V}(\overline{r}) = \overline{i}_z\, U_o\left[1 - \left(\frac{R}{R_o}\right)^2\right] \tag{2}$$

where the position vector $\bar{r}$ is expressed in the cylindrical coordinates (R, Φ, Z). Accordingly,

$$\bar{V}_{(o)} = \bar{i}_z\, U_o\left[1 - \frac{\beta^2}{R_o^2}\right] \tag{3}$$

$$[\nabla^2 \bar{V}]_{(o)} = -\,\bar{i}_z \cdot \frac{4U_o}{R_o^2} \tag{4}$$

Therefore, from Eq. 1, the drag force on the spheres is found to be:

$$\bar{F}_D = \bar{i}_z\, 6\,\pi\, a\,\mu\left[U_o\left(1 - \frac{\beta^2}{R_o^2}\right) - \frac{2}{3}\,U_o\left(\frac{a}{R_o}\right)^2\right] \tag{5}$$

The application of Faxen's law to the case of a small sphere (radius b) placed in the vicinity of a much larger spherical collector (radius a) with a uniform flow at infinity is now considered. As far as the small sphere is concerned, the undisturbed flow, $\bar{V}(\bar{r})$, is given by the Stokes solution for creeping flow of an unbounded fluid over a sphere of radius a. Thus, $\bar{V}(\bar{r})$ is given by:

$$\bar{V}(\bar{r}) = \frac{1}{2\mu}\,\nabla\,(r^2\, p_{-2}) + \frac{\bar{r}}{\mu}\,p_{-2} + \nabla\,\psi_{-2} + U\,i_z \tag{6}$$

where

$$p_{-2} = \frac{3}{2}\,\mu\,\frac{a\,U\,z}{r^3} \tag{7}$$

$$\psi_{-2} = \frac{1}{4}\,\frac{a^3\,z\,U}{r^3} \tag{8}$$

The z-component of $\bar{V}$ evaluated at the center of the small particle, (r, θ, ϕ), is found to be:

$$U_{(o)} = U\left\{1 - \left(\frac{a}{r}\right) + \frac{1}{4}\left(\frac{a}{r}\right)\left(1 - \frac{a^2}{r^2}\right)(1 - 3\cos^2\theta)\right\} \tag{9}$$

In particular, consider the case where the line of centers of particle and collector is parallel or perpendicular to the direction of the main flow. From Eq. 1 the z-components of the drag force on the particle in each respective case is given as:

$$(F_{D,p})_{\parallel} = 6\,\pi\, b\,\mu\, U\left\{1 - \frac{3}{2}\left(\frac{a}{l}\right) + \left(\frac{a}{l}\right)^3\right\} \tag{10}$$

and

$$(F_{D,p})_{\perp} = 6\,\pi\, b\,\mu\, U\left\{1 - \frac{3}{4}\left(\frac{a}{l}\right) - \frac{1}{2}\left(\frac{a}{l}\right)^3\right\} \tag{11}$$

where l is the center-to-center distance between the particle and the collector.

The total drag on the collector-particle system is given by:

$$F_{D,\text{total}} = 6\,\pi\, a\,\mu\, U + F_{D,p} \tag{12}$$

where

$$F_{D,p} = (F_{D,p})_{\parallel}\cdot\cos^2\theta + (F_{D,p})_{\perp}\sin^2\theta \tag{13}$$

and θ is the angle between the line of centers and the flow direction.

Eq. 12 yields results which are in fairly good agreement with the exact solution when $a = b$, and $l \gg (a + b)$ (i.e., two equal spheres far apart from each other) as shown in Table 1. However, when the attached particle is very small as compared to the collector ($b \ll a$, and $l = a + b$), it leads to spurious results, suggesting erroneously that the attached particle leads to a negative effect on the drag force, and that the total drag force acting on the collector-particle assembly is less than the drag force acting on the clean collector, Table 2. For example, with an attached particle at the $\theta = \pi/2$ position and $(b/a) = 0.05$, the total drag force, $F_{D,\text{total}}$ is given as $(F_{D,\text{total}}/6\,\pi\,\mu\, a\, U) = 0.99269$; thus, $(F_{D,p})_{\perp}/6\,\pi\,\mu\, a\, U) = -0.00731$.

TABLE 1. COMPARISON OF THE ESTIMATIONS BASED ON THE APPROXIMATE METHODS: TOTAL DRAG FORCE ON TWO EQUAL SPHERES AT VARIOUS SPACING $[F_{D,\text{total}}/(F_{D,a})_o]$

Spacing ($l/2a$)	Line of Centers Parallel to the Direction of Motion ($\theta = 0$)		Line of Centers Perpendicular to the Direction of Motion ($\theta = \pi/2$)	
	Exact solution	Eq. 12	Exact solution	Eq. 12
10	1.86072	1.9251	1.92760	1.9624
5	1.74120	1.8510	1.85962	1.9245
4	1.68824	1.8145	1.82696	1.9158
3	1.60944	1.7546	1.77418	1.8727
2	1.48452	1.6406	1.67360	1.8047
1	1.29028	1.3750	1.44938	1.5625
	Exact solution	Eq. 15	Exact solution	Eq. 15
10	1.8607	1.9251	1.9276	1.9625
5	1.7412	1.8505	1.8596	1.9248
4	1.6882	1.8135	1.8270	1.9058
3	1.6094	1.7523	1.7742	1.8738
2	1.4845	1.6328	1.6736	1.8086
1	1.2903	1.3125	1.4494	1.5938

The fact that Eq. 12 predicts a negative drag force, of course, is unacceptable. The need to modify Faxen's result, if possible, is therefore evident. The second term on the right hand side of Eq. 1, viewed as a correction term is, in general, smaller than the first term. Assuming that it can be ignored, $F_{D,p}$ will be given by:

$$F_{D,p} = 6\,\pi\,\mu\, b\, U_{(o)} \tag{14}$$

Eq. 14 is equivalent to the assumption that the drag force contribution of the attached particle is given by Stokes law with the approach velocity, U, replaced by the z-direction velocity component $U_{(o)}$, of the velocity field generated by the presence of the collector alone (Eq. 6).

The total drag on the collector-particle system is then:

$$F_{D,\text{total}} = 6\,\pi\, a\,\mu\, U + 6\,\pi\, b\,\mu\, U_{(o)} \tag{15}$$

where $U_{(o)}$ is given by Eq. 9.

The drag force contribution of the attached particle can then be written as follows:

$$\frac{\Delta F_{D,p}}{F_{D,a}} = \frac{F_{D,\text{total}} - F_{D,a}}{F_{D,a}} = \left(\frac{b}{a}\right)\left(\frac{U_{(o)}}{U}\right) \tag{16}$$

where $F_{D,a}$ is the drag force on the clean collector and

$$\frac{U_{(o)}}{U} = 1 - \left(\frac{a}{r}\right) + \frac{1}{4}\left(\frac{a}{r}\right)\left(1 - \frac{a^2}{r^2}\right)(1 - 3\cos^2\theta) \tag{17}$$

TABLE 2. COMPARISON OF THE TOTAL DRAG FORCE ESTIMATED FROM EQS. 12 AND 15

$F_{D,\text{total}}/(F_{D,a})_{\text{clean}}$

Size Ratio (b/a)	Line of Centers Parallel to the Direction of Motion ($\theta = 0$*)		Line of Centers Perpendicular to the Direction of Motion ($\theta = \pi/2$)	
	Eq. 12	Eq. 15	Eq. 12	Eq. 15
0.20	1.0657	1.0079	1.01713	1.046
1.10	1.0388	1.0012	1.99425	1.0130
0.05	1.0217	1.000167	0.99269†	1.00349
0.02	1.0094	1.0000115	0.99587†	1.00058
0.01	1.00485	1.0000015	0.99772†	1.00014

†Predictions of negative drag on the attached particle based on Faxen's law, yield the values of the total drag force on the collector particle assembly that are less than the drag on the clean collector.

where (r, θ, ϕ) are the position coordinates of the center of the particle in a spherical coordinate system with the origin at the collector center.

Eq. 15, therefore, provides a very simple procedure for the calculation of the drag force on the system of a single particle attached to a large spherical body. A comparison between the results of Eq. 15 and Eqs. 10, 11, 12, and 13 is given in Table 2. Eq. 15 gives a lower value than Eq. 12 when the line of centers is parallel to the direction of the main flow but gives higher values when the line of centers is perpendicular to the direction of the main flow. Furthermore, it does not predict the unacceptable negative effect when deposited particles are present. Eq. 15 was first used by Payatakes and Tien (1976). Its major deficiency is its lack of a sound theoretical basis. Its use, therefore, has to be justified by experimental evidence, as discussed in later sections.

Interaction among Deposited Particles

The case of a single particle attached to a spherical collector, of course, represents a limiting situation in the deposition process. A more realistic situation would involve the presence of a number of particles attached to the collector at various parts of the collector surface, Figure 1(b). If the deposited particles are widely separated, Eq. 14 can be used to estimate, as an approximation, the drag force contribution from the individual particles. The more general situation, however, requires consideration of the effect of interaction among these attached particles.

In accounting for the interaction effect, the simplest case is that of two attached particles. For such a case, the increase in drag force can be written as:

$$\Delta F_D = F_{D,\text{total}} - (F_{D,c})_o = \Delta F_{D,1} + \Delta F_{D,2} \tag{18}$$

$$\Delta F_{D,1} = (\Delta F_{D,1})_o \, f_{12}(\bar{r}_1, \bar{r}_2) \tag{19}$$

$$\Delta F_{D,2} = (\Delta F_{D,2})_o \, f_{21}(\bar{r}_1, \bar{r}_2) \tag{20}$$

$(\Delta F_{D,1})_o$ and $(\Delta F_{D,2})_o$ denote the contributions to drag force increase due to particles 1 and 2 when each one is attached singly; and $\Delta F_{D,1}$ and $\Delta F_{D,2}$ denote the contributions to the drag force increase due to particles 1 and 2 in presence of each other. $\bar{r}_1$ and $\bar{r}_2$ are the position vectors of the centers of the two particles. f_{12} and f_{21} denote the effect of particle 2 on particle 1 are vice versa.

Eqs. 14 and 15 are not suited for correlating the experimental data since it is difficult to measure $\Delta F_{D,1}$ and $\Delta F_{D,2}$ separately. The measurements performed in this work (see later sections) yield values of drag forces acting on clean collectors and on collectors with deposited particles, from which the increase in drag force can be obtained. Accordingly, it is more convenient to define an interaction factor in terms of this increase in drag force, ΔF_D, or

$$\frac{\Delta F_D}{(\Delta F_{D,1})_o + (\Delta F_{D,2})_o} = f(\bar{r}_1, \bar{r}_2) \tag{21}$$

Eq. 21 embodies the underlying assumption that the collector-particle interaction and particle-particle interaction can be combined and expressed by a single interaction function for two attached particles. The two-sphere interaction problem has been solved by both analytical and numerical methods. Based on Happel and Brenner's results (1973), one may write:

$$f(r_1, r_2) = f\left(\frac{l}{b}, \alpha\right) = \left[\left\{\frac{1}{1 + \frac{3}{2}\left(\frac{b}{l}\right) - \left(\frac{b}{l}\right)^3}\right\} \cdot \cos^2\alpha + \left\{\frac{1}{1 + \frac{3}{4}\left(\frac{b}{l}\right) + \frac{1}{2}\left(\frac{b}{l}\right)^3}\right\} \cdot \sin^2\alpha\right] \tag{22}$$

where l is the distance between two particles and α is the angle between the main flow and the line of centers of the particles. The validity of this expression will be checked against experimental results to be discussed in a later section.

For the more general case when N particles are attached to the collector with various degrees of proximity, interactions exist among all the particles. In analogy with Eqs. 18, 19 and 20, one may write:

$$\Delta F_D = \Delta F_{D,1} + \Delta F_{D,2} + \ldots \Delta F_{D,N} \tag{23}$$

$$\Delta F_{D,i} = (\Delta F_{D,i})_o \cdot f_i(\bar{r}_1, \bar{r}_2, \ldots \bar{r}_N) \tag{24}$$

In considering the interaction between the i-th attached particle and its neighbors, it is plausible that the dominant contribution is made by those closer to it than those farther away. Let the j-th attached particle be the closest to the i-th particle. As an approximation, one has:

$$f_i(\bar{r}_1, \bar{r}_2, \ldots \bar{r}_N) \simeq f(\bar{r}_i, \bar{r}_j) \tag{25}$$

where $f(\bar{r}_i, \bar{r}_j)$ is the interaction factor defined by Eq. 21 and given by Eq. 22.

Equally plausible, one may assume that the major interaction between the i-th particle and the other attached particles can be accounted for by including the interaction between the i-th particle and the two attached particles closest to it (say the j-th and the k-th). This interaction can be taken as the product of the interaction factors of the i-j pair and the i-k pair, or

$$f_i = f(\bar{r}_i, \bar{r}_j) \cdot f(\bar{r}_i, \bar{r}_k) \tag{26}$$

The utility of these two expressions (i.e., Eq. 25 and 26) will be evaluated by comparing them with experiments later.

Drag Force Contribution of an Ideal Dendrite of Particles.

The increase in the drag force due to the presence of a straight chain of particles, $(\Delta F_D)_{\text{dendrite}}$, Figure 1(c) can be estimated by comparing the collector-particle interaction and particle-particle interaction as follows. Let

$$\frac{(\Delta F_D)_{\text{dendrite}}}{\sum_{i=1}^{n} (\Delta F_{D,i})_o} = f_{\text{dendrite}}(n, \alpha) \tag{27}$$

where f_{dendrite} denotes the function accounting for the interaction of the particles constituting the dendrite; n is the number of particles in the dendrite; α is the angle between the dendrite and the main flow $(\Delta F_{D,i})_o$ denotes the contribution to drag force increase of each individual particle if it were present alone. $(\Delta F_{D,i})_o$, therefore, can be estimated from the modified Faxen's law for collector-particle interaction (i.e., Eq. 16).

The particle-particle interaction is approximated by the hydrodynamic interaction among a finite number of equal-sized spheres attached to each other to form a straight chain in creeping flow field. Ganatos et al. (1978) and Gluckman et al. (1971) have considered the problem of flow over straight particle chains composed of very closely spaced spheres of equal size.

In the case of seven spheres with interparticle clearance of 0.0025 sphere diameters, the drag force correction factor ranges from 0.41 for the central sphere to 0.51 for the outermost one when the main flow is perpendicular to the chain. The mean correction factor for the chain is 0.44. For the case of parallel flow, the drag force correction factor for the central sphere is 0.25 and that for the outermost one is 0.56. The mean correction factor in this case is 0.325 (Gluckman, Pfeffer and Weinbaum, 1971). As the number of particles in the chain approaches infinity, the drag force correction factor $\lambda_{\parallel}$ approaches zero. For a case of 101 touching spheres in a chain, with the main flow parallel to the chain, the drag correction factor is found to be 0.15 (Gluckman et al., 1971). For a case with the main flow perpendicular to the chain, the corresponding value is 0.30, as $(\lambda_{\perp}/\lambda_{\parallel})$ is approximately 2 (Ganatos et al., 1978).

Based on these results for the interaction of particles in a chain, f_{dendrite} is assumed to have the following typical values:

For $\alpha = 0^*$, i.e., the main flow parallel to the chain,

$$f_{\text{dendrite}}\ (2,\ 0^*) = 0.645$$

$$f_{\text{dendrite}}\ (7,\ 0^*) = 0.325 \qquad (28)$$

$$f_{\text{dendrite}}\ (101,\ 0^*) = 0.15$$

and for $\alpha = \pi/2$, i.e., the main flow perpendicular to the chain,

$$f_{\text{dendrite}}\ (2,\ \pi/2) = 0.724$$

$$f_{\text{dendrite}}\ (7,\ \pi/2) = 0.44 \qquad (29)$$

$$f_{\text{dendrite}}\ (101,\ \pi/2) = 0.30$$

An approximate representation of these results is given by:

$$f_{\text{dendrite}}\ (n,\ \alpha) =$$

$$[(\cos^2 \alpha) \cdot \{0.7 - 0.05n\} + (\sin^2 \alpha) \cdot \{0.8 - 0.05n\}] \qquad (30)$$

$$\text{for } 2 \le n \le 10$$

with $f_{\text{dendrite}}\ (1,\ \alpha)$ is identically equal to unity.

A comparison of this relationship with experimental data is presented in subsequent sections.

EXPERIMENTAL STUDY

Principle and Design of Experiment: The experimental work consists of the measurement of the hydrodynamic drag force acting on sphere-particle assemblies similar to those shown in Figure 1, when subjected to slowly moving viscous fluid. The method relies on the capability of an electrobalance to detect small changes in the effective weight of the sphere-particle assembly caused by the drag force acting on it. The drag force acting on the assembly, F_D, is given by:

$$F_D = W_o - W \qquad (31)$$

where W_o is the weight of the test assembly when submerged in a stationary fluid; W is the weight when the assembly is subjected to an upward flow of fluid.

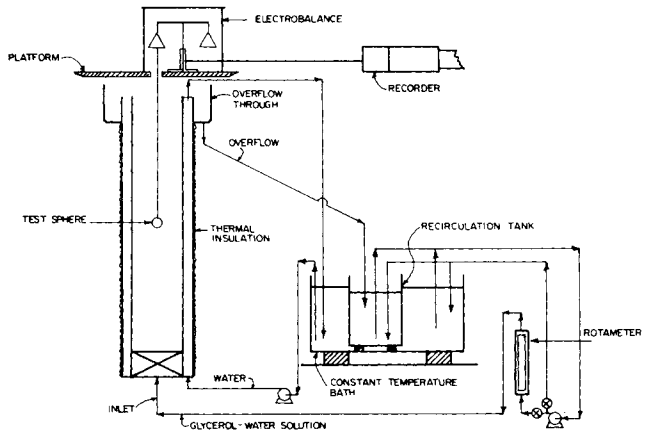

Figure 2. Schematic diagram of the experimental set-up for drag force measurements.

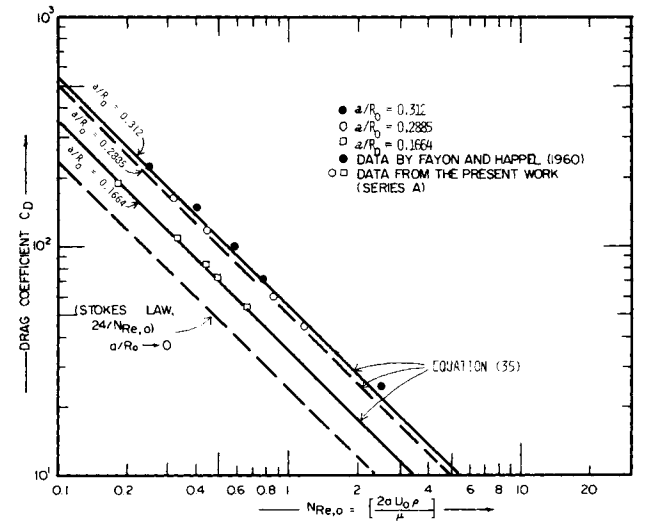

Figure 3. Drag force on a sphere placed at the cylinder axis.

Experimental Apparatus: The schematic diagram of the experimental apparatus is shown in Figure 2. The main components of the experimental apparatus are a water tunnel, a recirculation tank and an electrobalance.

The water tunnel was made of a 180 cm long Plexiglass cylinder with 13.355 cm internal diameter. The column was encased in an outer plexiglass cylinder (I.D. 22.225 cm) which served as a constant temperature jacket. The outer jacket was covered with fiberglass thermal insulation (5 cm in thickness) in order to minimize the effect of ambient temperature variations. The bottom of the water tunnel was packed with glass rings, 10 mm in diameter and 10 mm long, to a height of 14 cm to reduce the jetting effect of the entering fluid, and to ensure that a fully developed Poiseullian flow obtained in the middle section of the tunnel.

A 3.85 cm diameter steel ball was used as the spherical collector. Various configurations of sphere-particle assemblies were made by attaching small steel balls (with diameters of 0.635, 0.7525, 1.27 and 1.5875 cm) onto the surface of the collector using superglue (commercially available). A sufficiently long thin steel wire (0.04 cm in diameter) was silver soldered to the test sphere. The sphere particle assembly is suspended from the pan of the electrobalance (Ainworth Type 15 with ±0.5 mg accuracy) and mounted on the platform above the water tunnel. The balance was so positioned that the center of the suspended collector was on the cylinder axis.

The circulating fluid flowing through the water tunnel was made up of 92% glycerol in water solution (viscosity of 0.21 Pa · s at 298 K). It entered the bottom of the tunnel and returned to the recirculation tank from the overflow trough provided at the top of the tunnel. The recirculation tank was equipped with a temperature control system consisting of cooling coils, heaters, thermoregulators (Mercury column type) and electronic relay. Thermometers were provided in the tank and at the top of the water tunnel. A submersible pump, provided with a bypass and control valve was used for the fluid circulation. The fluid temperature in the tunnel was kept constant within 0.5 K. The flow rate measurement was made with a rotameter (Type 1307-09 ERAIE).

Experimental Procedure: A run was begun by connecting the sphere particle assembly to the pan of the balance with the fluid at rest in the tunnel. The fluid maintained at a specified temperature (298 K) was then circulated at a desired flowrate. The weight of the sphere-particle assembly was recorded separately with fluid flow on and off. The difference in weight is the drag force acting on the test assembly due to fluid motion.

Results: The body of experiments performed in this work can be classified as follows:

SERIES A RUNS:

Measurement of drag force on a clean test sphere.

(1) collector diameter: 3.85 cm, 2.2225 cm
(2) flow rate: 34.5, 26.3, 18.0 9.9 cm^3/s

SERIES B RUNS:

Measurement of drag force on a test sphere with a single attached particle.

(1) collector diameter: 3.85 cm
(2) flow rate: 34.5 cm^3/s
(3) particle diameter: 0.635, 0.9526, 1.27 and 1.5875 cm
(4) particle position (θ): π, ($\pi/2$), ($\pi/4$), and ($3\pi/4$)

SERIES C RUNS:

Measurement of drag force on a test sphere with two attached particles.

(1) collector diameter: 3.85 cm
(2) flow rate: 34.5 cm^3/s
(3) particle diameter = 0.635, 0.9526, 1.27 and 1.5875 cm
(4) two particles attached at various interparticle spacing

SERIES D RUNS:

Measurement of contribution on a test sphere with a single attached particle dendrite.

(1) collector diameter: 3.85 cm.
(2) flow rate: 34.5 cm^3/s
(3) particle diameter = 0.635, 0.9526 and 1.27 cm
(4) number of particles in chain: 3, 4, 5, and 6
(5) position of the chain, (θ) = π, ($3\pi/4$)

SERIES E RUNS:

Measurement of drag force on a single test sphere with particle clusters attached to it with various configurations.

TABLE 3. EFFECT OF THE CYLINDRICAL WALL ON THE DRAG FORCE ACTING ON A SPHERE AT THE AXIS

$(a/R_o) = 0.2885$		$(a/R_o) = 0.1667$	
$N_{Re,o}$	$F_D/6\pi a\mu U_o$	$N_{Re,o}$	$F_D/6\pi a\mu U_o$
1.12	2.14	0.647	1.49
0.855	2.13	0.493	1.45
0.584	2.15	0.337	1.50
0.318	2.11	0.184	1.46
Predicted by Eq. 35	2.13	Predicted by Eq. 35	1.49

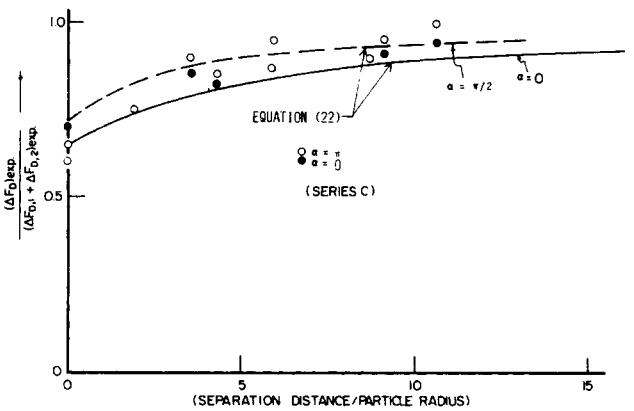

Figure 5. Drag force increase due to two attached particles.

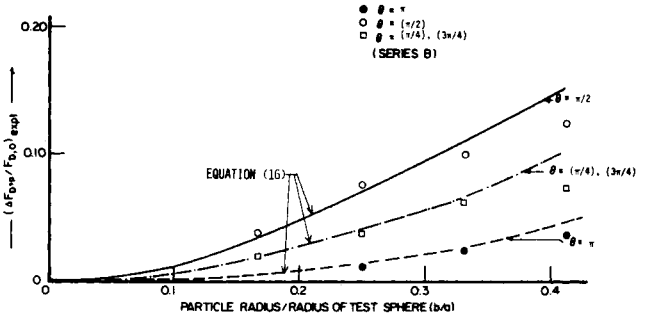

Figure 4. Drag force increase due to a single attached particle.

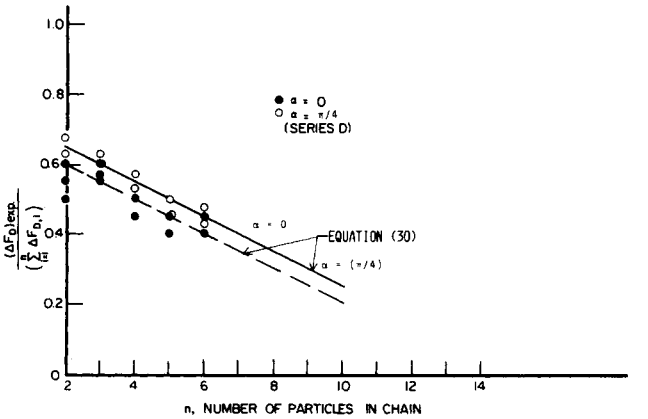

Figure 6. Drag force due to attached particle chain.

(1) collector diameter: 3.85 cm
(2) flow rate: 34.5 cm³/s
(3) particle diameter: 0.635 cm
(4) total number of particles: 10, 15
(5) configuration type: Fig. 1(b), (c) and (d)

The results of Series A measurements are used to establish the wall effect of the water tunnel and to check the accuracy of the electron microbalance measurements. Series B measurements are intended to check the validity of the drag force expression from the modified Faxen's law, i.e., Eq. 15. The extent of the interaction between the two attached particles, defined by Eq. 21 can be determined from the data collected from Series C measurements. The results of Series D measurements are used to establish the procedure for estimating the drag force acting on a spherical collector with a string of particles attached to it. From these measurements, a general procedure for estimating the drag force for a spherical collector with particles and/or particle clusters, attached to it is established, and then their validity is checked against the results of experiments in Series E.

Wall Effect: The effect of the water tunnel wall on the drag force experienced by a clean test sphere was examined using data from the Series A experiments, which are shown in Figure 3 in the form of the drag coefficient, C_D, against the Reynolds number $N_{Re,o} \cdot C_D$ and $N_{Re,o}$ are defined by:

$$C_D = \frac{F_D}{(\pi a^2)\left(\frac{\rho U_o^2}{2}\right)} \tag{32}$$

$$N_{Re,o} = \frac{2aU_o\rho}{\mu} \tag{33}$$

Also included in Figure 3 are the earlier data of Fayon and Happel (1960) and the C_D vs. $N_{Re,o}$ relationship based on Stokes law, i.e.:

$$C_{D,s} = \frac{24}{N_{Re,o}} \tag{34}$$

The consistency of the data can be seen from the fact that the C_D vs. N_{Re} curve approaches that given by Stokes law as the value of a/R_o diminishes.

The empirical expression for the drag force experienced by a sphere placed at the axis of a cylindrical tube, proposed by Fayon and Happel, is given by:

$$\frac{F_D}{6\pi\mu a U_o} = \frac{1 - \frac{2}{3}\left(\frac{a}{R_o}\right)^2}{1 - 2.105\left(\frac{a}{R_o}\right) + 2.807\left(\frac{a}{R_o}\right)^3} \tag{35}$$

A comparison of the experimental data and Eq. 35 is given in Table 3. The agreement is within 3% or better. This comparison, together with the results shown in Figure 3 demonstrate that the experimental apparatus used in this study yields accurate and reliable data.

Drag Force Increases Due to Single Attached Particles: Series B measurements were made on an assembly consisting of the test sphere with a particle attached to its surface at various positions, corresponding to $\theta = (\pi/4), (\pi/2), (3\pi/2)$ and π. The main flow was in the direction of $\theta = 0$. Measurements for particles located at $\theta = 0$ were not possible due to the presence of the suspension wire. Figure 4 shows the increase in the drag force due to the attached particle ($\Delta F_{D,p}$), as a function of the size of the particle for various positions. Comparisons of these measurements with the predictions based on the modified Faxen's law (Eq. 15) indicate that the agreement is fairly good; especially when the relative size of the particle, with respect to the test sphere, is small. The ratio of particle to collector radius commonly encountered in filtration, is of the order, $(b/a) < 0.05$. Thus for the case of a small particle attached to a large sphere, Eq. 15 or alternatively Eq. 16 may be used for the prediction of the drag force increase due to the attached particle.

Interaction Among Attached Particles: The Series C measurements for the drag force increase were taken for the case of two equal-sized particles attached to the test sphere. These data are shown in Figure 5 in the form of the ratio of the contribution of the drag force increase due to the two attached particles to the sum of the increases due to each of the two attached particles individually. The latter quantity was obtained from Series B measurements.

The distance between the two attached particles ranged from zero to fifteen times the particle radii. The separation distance is measured along the arc parallel to the collector surface and not the linear center to center distance. Also shown in Figure 5 are the results calculated from Eq. 22 for $\alpha = 0$ or $(\pi/2)$. It is clear that the discrepancy between the values of the interaction function $f(\bar{r}_1, \bar{r}_2)$ calculated from Eq. 22 and

TABLE 4. DETAILS OF THE CONFIGURATION OF ATTACHED PARTICLES (PARTICLE RADIUS/RADIUS OF TEST SPHERE) = 0.1649
CONFIGURATION NUMBER 1 AND 2

Particle Number i	Position of Particle Center (r/a)	θ	ϕ	$\Delta F_{D,p}/F_{D,o}$ Eq. 16	Experimental $\Delta F_D/F_{D,o}$	Corrected $(\Delta F_{D,p})/F_{D,o}$ for the effect of 1 Particle	2 Particles
1	1.1649	$\pi/2$	0	0.03265		0.02841	0.02471
2	1.1649	$\pi/2$	$\pi/2$	0.03265		0.02841	0.02471
3	1.1649	$\pi/2$	π	0.03265		0.02841	0.02471
4	1.1649	$\pi/2$	$3\pi/2$	0.03265		0.02841	0.02471
5	1.1649	$3\pi/4$	0	0.01869		0.01626	0.01414
6	1.1649	$3\pi/4$	$\pi/2$	0.01869		0.01626	0.01414
7	1.1649	$3\pi/4$	π	0.01869		0.01626	0.01414
8	1.1649	$3\pi/4$	$3\pi/2$	0.01869		0.01626	0.01414
9	1.1649	π	0	0.00472		0.00411	0.01414
10	1.1649	0.28	0	0.00692		0.00643	0.01414
Subtotal				0.21700	0.175	0.1892	0.165
11	1.1649	$\pi/4$	0	0.01869		0.01626	0.01414
12	1.1649	$\pi/4$	1.26	0.01869		0.01626	0.01414
13	1.1649	$\pi/4$	2.51	0.01869		0.01626	0.01414
14	1.1649	$\pi/4$	3.77	0.01869		0.01626	0.01414
15	1.1649	$\pi 4$	5.03	0.01869		0.01626	0.01414
Total				0.31045	0.2372	0.2705	0.2357

those based on the experimental data is within the experimental error. It also appears that if the distance between the two particles exceeds 10 times the particle radius, the effect of particle-particle interaction is negligible.

Drag Force Contribution of Ideal Particle Dendrites: Series D measurements provide experimental data for the drag force contribution due to the presence of a straight particle chain attached to the test sphere. The string of particles was attached at the front stagnation point ($\theta = \pi$) and at $\theta = 3\pi/4$. The number of particles in a chain ranged from 2 to 6. The comparison of the drag force increases due to the attached particle chains with the sum of individual contributions based on Eq. 16 as a function of the number of particles is shown in Figure 6.

The relative reduction in the drag force increases with the increase of the number of particles in the chain is clearly indicated, and agrees with the prediction of Eq. 30.

Drag Force Increase Due to Particle Clusters: Series E measurements were made using collectors with a number of attached particles and particle chains. Six specific configurations were used, and the details of these configurations (i.e., positions of individual particles) are given in Tables 4 to 6.

A comparison between the experimentally determined values of drag force increase and those predicted from Eq. 25 and 26 are also presented in Tables 4 to 6. The values of $(\Delta F_{D,i})_0$ are obtained from Eq. 16 and the interaction factors are estimated from Figure 5. In all six cases, the prediction according to Eq. 26 yields better results than Eq. 25.

The use of either Eqs. 25 or 26 is of course arbitrary. One can argue that the interaction effect should be considered in terms of those between the i-th particle and the three particles closest to it instead of only one or two. In fact, the argument can be extended to include all the $(N\text{-}1)$ particles in the cluster. In Table 7, the results obtained by considering the interaction between the i-th particle and the 'm' other particles closest to it with $m = 0, 1, 2, 3$, are tabulated and compared with data of Series E measurements. For the case of a dendrite forming a part of a particle cluster attached to the collector (configurations numbers 3 and 4), use of correction factors based on Eq. 30 to estimate the increase in drag force due to the particles in the dendrite, instead of Eq. 25 or Eq.

TABLE 5. DETAILS OF THE CONFIGURATION OF ATTACHED PARTICLES (PARTICLE RADIUS/RADIUS OF TEST SPHERE) = 0.1649
CONFIGURATION NUMBER 3 AND 4

Particle Number i	Position of Particle Center (r/a)	θ	ϕ	$\Delta F_{D,p}/F_{D,o}$ Eq. 16	Experimental $\Delta F_D/F_{D,o}$	Corrected $(\Delta F_{D,p})/F_{D,o}$ for the effect of 1 Particle	2 Particles
1	1.1649	$\pi/2$	0	0.03265		0.02841	0.02642
2	1.1649	$\pi/2$	$\pi/2$	0.03265		0.0304	0.02827
3	1.1649	$\pi/2$	π	0.03265		0.02841	0.02642
4	1.1649	$\pi/2$	$3\pi/2$	0.03265		0.0304	0.02827
5	1.1649	π	0	0.00472		0.00304	0.0022
6	1.4147	π	0	0.02411		0.01555	0.0100
7	1.8245	π	0	0.04290		0.02767	0.0178
8	1.8245	π	0	0.05833		0.03763	0.0271
9	1.1649	$3\pi/4$	0	0.01869		0.01626	0.01414
10	1.1649	$3\pi/4$	π	0.01869		0.01626	0.01414
Subtotal				0.2980	0.20	0.234	0.1925
11	1.4947	$3\pi/4$	0	0.04696		0.0303	0.0264
12	1.4947	$3\pi/4$	π	0.04696		0.0303	0.0264
13	1.1649	$\pi/4$	0	0.01869		0.01205	0.0112
14	1.1649	$\pi/4$	π	0.01869		0.01626	0.01514
15	1.1649	$\pi/4$	0.35	0.01869		0.01205	0.0105
Total				0.4480	0.2875	0.334	0.282

TABLE 6. DETAILS OF THE CONFIGURATION OF ATTACHED PARTICLES (PARTICLE RADIUS/RADIUS OF TEST SPHERE) = 0.1649 CONFIGURATION NUMBER 5 AND 6

Particle Number i	Position of Particle Center (r/a)	θ	ϕ	$\Delta F_{D,p}/F_{D,o}$ Eq. 16	Experimental $\Delta F_D/F_{D,o}$	Corrected $(\Delta F_{D,p})/F_{D,o}$ for the effect of 1 Particle	2 Particles
1	1.1649	π	0	0.00472		0.00304	0.00196
2	1.1649	2.86	0	0.00692		0.00446	0.00287
3	1.1649	2.86	$\pi/3$	0.00692		0.00446	0.00287
4	1.1649	2.86	$2\pi/3$	0.00692		0.00446	0.00287
5	1.1649	2.86	π	0.00692		0.00446	0.00287
6	1.1649	2.86	$4\pi/3$	0.00692		0.00446	0.00287
7	1.1649	2.86	5.24	0.00692		0.00446	0.00287
8	1.1649	2.58	0	0.01281		0.00826	0.00533
9	1.1649	2.58	$\pi/2$	0.01281		0.00826	0.00533
10	1.1649	2.48	$3\pi/2$	0.01281		0.00826	0.00533
Subtotal				0.0847	0.0375	0.0546	0.0352
11	1.4977	2.86	0	0.0277		0.01786	0.0115
12	1.4947	2.86	$\pi/3$	0.0277		0.01786	0.0115
13	1.4947	2.86	$2\pi/3$	0.0277		0.01786	0.0115
14	1.4947	2.86	π	0.0277		0.01786	0.0115
15	1.4947	2.86	$4\pi/3$	0.0277		0.01786	0.0115
Total				0.2232	0.0875	0.144	0.0929

26 yields marginal improvement in the prediction, Table 7. The results suggest that use of only two of the closest particles yields optimum results.

RECOMMENDED PROCEDURE FOR CALCULATING DRAG FORCE CONTRIBUTION

The experimental data obtained in this work confirm the validity of the simple expression developed on the basis of Faxen's law and other theories for the drag force on the multiparticle systems. The results can be summarized as follows.

(a) The drag force increase due to the presence of a single deposited particle of radius b is given by:

$$\Delta F_{D,p} = 6\pi b\mu U_{(o)} \tag{32}$$

where $U_{(o)}$ for a spherical collector is given by Eq. 17. In general, $U_{(o)}$ is the velocity component along the direction of the main flow evaluated at the center of the deposited particle from the velocity field around the clean collector.

(b) The drag force increase due to the presence of a particle chain can be estimated from Eq. 30.

(c) Effects of other attached particles on the contribution to the drag force increase due to a given particle can be ignored if the separation distance between the particles is greater than 10 particle radii.

(d) The reduction in the contribution to drag force increase by a given particle due to another attached particle can be estimated by Eq. 22.

(e) In the case of clusters of attached particles, the contribution to the increase in drag force attributable to a given particle can be estimated by correcting the individual contribution for that particle given by Eq. 16 for the interaction effect due to only the two closest neighboring attached particles, using Eqs. 22 and 26. This is an adequate approximation accounting for the interaction effects of all the neighboring particles.

ESTIMATION OF PRESSURE DROP INCREASE ACROSS CLOGGED FILTER BED

The results obtained in this work can be readily used to estimate the pressure drop increase across clogged filter beds. The pressure drop associated with the flow through a porous medium represents the cumulative drag forces acting on the surface of the medium matrix. Thus with the use of the single collector model representing medium, the fractional increase in pressure drop is equal to the fractional increase in drag force contributed by deposited particles, or

$$\frac{\Delta p}{\Delta p_o} - 1 = \frac{1}{F_{D_o}} \sum_{i=1}^{N} \Delta F_{D_i} \tag{33}$$

where Δp and Δp_o are the pressure drop corresponding to the clogged and clean filter, respectively. F_{D_o} is the drag force acting on the clear collector. ΔF_{D_i} are the drag force contribution due to the i-th deposited particle on the collector. There are N particles deposited on the collector.

TABLE 7. PREDICTION OF THE TOTAL DRAG FORCE INCREASE DUE TO PARTICLES ATTACHED IN VARIOUS CONFIGURATIONS

Configuration No.	Number of Particles	$(\Delta F_D/F_{D,o})$ expt	$(\Delta F_D/F_{D,o})$, Predicted with Correction for the Effect of m Other Particles $m = 0$	$m = 1$	$m = 2$	$m = 3$	$(\Delta F_D/F_{D,o})$, Predicted Using Eq. 30 for the Effect of the Dendrite
1	10	0.175	0.217	0.189	0.165	0.144	
2	15	0.2372	0.3105	0.271	0.236	0.206	
3	10	0.20	0.298	0.234	0.193	0.158	0.203
4	15	0.2875	0.448	0.334	0.282	0.238	0.290
5	10	0.0375	0.0847	0.0546	0.0352	0.0227	
6	15	0.0875	0.2232	0.144	0.0929	0.0599	

The estimation of the values of ΔF_{D_i} can be made with the procedure described above. To make these estimations, it is necessary to have the detailed knowledge about the morphology of deposited particles; namely, the positions of each deposited particle. Such information can be obtained with the simulation model developed recently (Tien et al., 1977; Wang et al., 1977).

ACKNOWLEDGEMENT

This study was performed under Grant No. 79-05962, National Science Foundation.

NOTATION

a = Collector radius
b = Particle radius
C_D = Drag coefficient, Eq. 32
$C_{D,s}$ = Drag coefficient based on Stokes' law, Eq. 34
$f(\bar{r}_i, \bar{r}_j)$ = drag correction factor for the interaction between the i-th and j-th particles
$f(\bar{r}_1, \bar{r}_2 \ldots \bar{r}_N)$ = drag correction factor for the interaction among the N particles
$f_{\text{dendrite}}(n, \alpha)$ = drag correction factor for particle dendrite
F_D = Drag force
$F_{D,i}$ = Drag force on the i-th sphere
ΔF_D = Increase in drag force, Eq. 18
$\Delta F_{D,i}$ = Contribution to drag force increase due to the i-th particle
l = Center to center distance between two spheres
$N_{Re,o}$ = Reynolds number, $(2\ a\ U_o\ \rho/\mu)$
p = Pressure
p_{-n-1} = Spherical harmonic function of order $(n + 1)$
ΔP = Pressure drop
$\bar{r}$ = position vector in cylindrical polar coordinate
R_0 = Radius of cylinder
R = radial coordinate
U = Approach velocity
U_o = Fluid velocity at cylinder axis
$U_{(o)}$ = z component of the undisturbed velocity field evaluated at the center of the particle, Eq. 9
$\bar{V}$ = Velocity field
W = Weight of the assembly subject to fluid flow
W_o = Weight of the assembly placed in fluid at rest
z = axial coordinate

LITERATURE CITED

Beizaie, M., "Deposition of Particles on a Single Collector," Ph.D Dissertation, Syracuse University, Syracuse, NY (1977).

Fayon, A. M., and J. Happel, "Effect of a Cylindrical Boundary on a Fixed Rigid Sphere in a Moving Viscous Fluid," *AIChE J.*, 6 (1960).

Ganatos, P., R. Pfeffer, and S. Weinbaum, "A numerical solution technique for Three-Dimensional Stokes' Flows with Application to the Motion of Strongly Interacting Spheres in a Plane," *J. Fluid Mech.*, **84**, 79 (1978).

Gluckman, M. J., R. Pfeffer, and S. Weinbaum, "A New Technique for Treating Multiparticle Slow Viscous Flow: Axisymmetric Flow Past Spheres and Spheroids," *J. Fluid Mech.*, **50**, 705 (1971).

Goldman, A. J., R. G. Cox, and H. Brenner, "The Slow Motion of Two Identical Arbitrarily Oriented Spheres Through a Viscous Fluid," *Chem. Eng. Sci.*, **21**, 1151 (1966).

Happel, J., and H. Brenner, "Low Reynolds Number Hydrodynamics," 2nd ed., Nordhoff, Leydeon (1973).

Lin, C. J., K. J. Lee, and N. S. Sather, "Slow Motion of Two Spheres in a Shear Flow," *J. Fluid Mech.*, **43**, 35 (1970).

Nir, A., and A. Acrivos, "On Creeping Motion of Two Arbitrary Sized Touching Spheres in a Linear Shear Field," *J. Fluid Mech.*, **43**, 35 (1970).

O'Neill, M. D., "On Asymmetric Slow Viscous Flows Caused by Motion of Two Equal Spheres Almost in Contact," *Proc.*, Camb. Phill. Soc., **65**, 543 (1969).

Payatakes, A. C., and C. Tien, "Particle Deposition in Fibrous Media with Dendrite-like Pattern: A Preliminary Model," *J. Aerosol Sci.*, **7**, 85 (1976).

Pendse, H., "A Study of Certain Problems in Deep Bed Filtration," Ph.D. Dissertation, Syracuse University, Syracuse, NY (1979).

Stimson, M., and G. B. Jeffery, "The Motion of Two Spheres in a Viscous Fluid," *Proc.*, Roy. Soc. (London), **A111**, 110 (1926).

Stokes, C. G., "On the Effect of the Internal Friction of Fluids on the Motion of Pendulums," *Trans.*, Cambr. Phill. Soc., **9**, pt. II, 8 (1851).

Tien, C., C. S. Wang, and D. T. Barot, "Chain-like Formation of Particle Deposits in Fluid Particle Separation," *Science*, **196**, 983 (1977).

Wang, C. S., M. Beizaie and C. Tien, "Deposition of Solid Particles on a Collector: Formulation of a New Theory," *AIChE J.*, **23**, 879 (1976).

Manuscript received February 26, 1980; revision received July 21, and accepted July 25, 1980.

Laminar Condensation Heat and Mass Transfer to a Moving Drop

J. N. CHUNG

and

P. S. AYYASWAMY

University of Pennsylvania
Philadelphia, Pennsylvania 19104

This paper presents numerical solutions to the nonlinear, coupled boundary-layer equations governing laminar condensation heat and mass transfer in the vicinity of the forward stagnation point of a spherical cold water droplet translating in a saturated mixture of three components. The environment surrounding the droplet is composed of a condensable (steam), a noncondensable and nonabsorbable (air), and a third component which is noncondensable but absorbable (Elemental Iodine, for example). The dispersed and the continuous phases have been treated simultaneously. Results obtained here show excellent agreement with experimental results where available. An important conclusion is that for laminar condensation on a freely falling droplet, for a given thermal driving force and noncondensable gas concentration in the bulk, the dimensionless heat transfer decreases with increasing saturation temperature of the outside medium.

SCOPE

In an earlier paper, Chung and Ayyaswamy (1978a) (hereinafter referred to as I) we have provided results for the forward stagnation point heat and mass transfer to a moving drop in the presence of laminar condensation. The theoretical development invoked two major simplifying assumptions. (a) The droplet inside could be treated as completly inviscid. Thus, the flow field inside the droplet was prescribed. The effect of

J. N. Chung is presently with the Department of Mechanical Engineering, Washington State University, Pullman, Washington 99163.

0001-1541-81-4381-0372-$2.00.